Observations of Kolmogorov Turbulence in Saturn's Magnetosphere

S B Xu, S Y Huang, Fouad Sahraoui, Z G Yuan, H H Wu, K. Jiang, J. Zhang, R T Lin

Geophysical Research Letters

RESEARCH LETTER
10.1029/2023GL105463

Observations of Kolmogorov Turbulence in Saturn's Magnetosphere

S. B. Xu[1], S. Y. Huang[1], F. Sahraoui[2], Z. G. Yuan[1], H. H. Wu[1], K. Jiang[1], J. Zhang[1], and R. T. Lin[1]

[1]School of Electronic Information, Hubei Luojia Laboratory, Wuhan University, Wuhan, China, [2]Laboratoire de Physique des Plasmas, CNRS-Ecole Polytechnique-Sorbonne Université-Paris-Saclay-Observatoire de Paris-Meudon, Palaiseau, France

Key Points:

- Magnetic field and electron density spectra have Kolmogorov scaling of $f^{-5/3}$ at MHD scales in Saturn's magnetosphere
- The spatial distribution of the Kolmogorov spectra within Saturn's magnetosphere reveals the extensive occurrence of Kolmogorov-like events
- The fluctuations for Kolmogorov-like events are dominated by Alfvénic modes (44.64%) with respect to magnetosonic-like one (6.94%)

Correspondence to:
S. Y. Huang,
shiyonghuang@whu.edu.cn

Citation:
Xu, S. B., Huang, S. Y., Sahraoui, F., Yuan, Z. G., Wu, H. H., Jiang, K., et al. (2023). Observations of Kolmogorov turbulence in Saturn's magnetosphere. *Geophysical Research Letters*, *50*, e2023GL105463. https://doi.org/10.1029/2023GL105463

Received 12 JUL 2023
Accepted 28 JUL 2023

Abstract The Kolmogorov scaling in the inertial range of scales is a distinct characteristic of fully developed turbulence, and studying it offers valuable insights into the evolution of turbulence. In this work, we perform a statistical survey of the power spectra with the Kolmogorov scaling in Saturn's magnetosphere using Cassini measurements. Two cases study show that both magnetic-field and electron density spectra exhibit $f^{-5/3}$ at the MHD scales. The statistical analysis reveals a wide-ranging and abundant presence of Kolmogorov spectra throughout magnetosphere, observed across all local times. Interestingly, the occurrence rate of these Kolmogorov-like events within Saturn's magnetosphere surpasses that observed in the planetary magnetosheath. The measurements of magnetic compressibility for the Kolmogorov-like events show the dominance of incompressible Alfvénic turbulence (44.64%) with respect to magnetosonic-like one (6.94%). In addition, the source and evolution of the turbulent fluctuations are further discussed.

Plain Language Summary Turbulence is ubiquitous in space and astrophysical plasmas, such as the solar wind, planetary magnetospheres, and the interstellar medium. Plasma turbulence has been widely studied in the solar wind and planetary magnetosheaths, but much less in the planetary magnetospheres. In the solar wind, power spectral density of the magnetic field fluctuations generally follows the so-called Kolmogorov spectrum $f^{-5/3}$ at the magnetohydrodynamic (MHD) scales, which suggests a fully developed turbulent state. In this study, we have discovered the widespread presence of Kolmogorov spectra in the Saturn's magnetosphere. The spatial distribution and nature of turbulent fluctuation for the Kolmogorov-like events are also investigated in detail.

1. Introduction

Turbulence is ubiquitous in space plasmas such as the solar wind, planetary plasma environments and the interstellar medium (e.g., Bruno & Carbone, 2013; Tu & Marsch, 1995). Due to the high-quality data provided by many recent spacecraft missions, plasma turbulence has been studied in the solar wind (e.g., Horbury et al., 2008; Huang et al., 2021; Huang & Sahraoui, 2019; Matthaeus & Goldstein, 1982a; Sahraoui et al., 2009, 2010, 2013; Wu et al., 2019, 2020, 2021; Zhang et al., 2022), the magnetosheath and the magnetospheres of solid planets (e.g., Andrés et al., 2020; He et al., 2011; Huang, Zhang et al., 2020; Huang et al., 2012, 2014, 2017; Sahraoui et al., 2003, 2006; Vörös et al., 2004, 2006, 2008; Zhang et al., 2023) and giant planets (e.g., Hadid et al., 2015; Saur, 2021; Tao et al., 2015; von Papen and Saur, 2016; von Papen et al., 2014). Similarities and differences in the turbulence properties in some of those media have been discussed in Sahraoui et al. (2020) and S. Y. Huang (2022).

Kolmogorov theory predicts that the power spectral density of the fluctuations obeys a $k^{-5/3}$ power-law in the inertial range (Kolmogorov, 1941). This theory was later extended to magnetohydrodynamic (MHD) turbulence leading to similar prediction on the scaling law, which spectrum has been routinely observed in the solar wind in the frequency range [10^{-4}, 10^{-1}] Hz (Bale et al., 2005; Bandyopadhyay, Chasapis, Chhiber, Parashar, Maruca, et al., 2018; Bandyopadhyay, Chasapis, Chhiber, Parashar, Matthaeus, et al., 2018; Bruno & Carbone, 2013; Coleman, 1968; Goldstein et al., 1994; Matthaeus & Goldstein, 1982a; Sahraoui et al., 2009, 2013). At lower frequencies ($<10^{-4}$ Hz), the spectra generally flatten to $\sim f^{-1}$; the corresponding range is referred to as the energy-containing scales (Bavassano et al., 1982). Different theoretical interpretations were given to explain the *1/f* spectrum (Chandran, 2018; Matteini et al., 2019; Matthaeus & Goldstein, 1986). At higher ($>10^{-1}$ Hz), the turbulence spectra were found to steepen significantly because of the joint action of dispersive and dissipation

effects (Goldstein et al., 1995; Howes et al., 2011; Huang et al., 2022; Huang & Sahraoui, 2019; Leamon et al., 1998; Sahraoui et al., 2009, 2010, 2013, 2013; Schekochihin et al., 2009; Wu et al., 2022). Such dissipation is thought to result into particle heating and acceleration in the solar wind.

Planetary magnetosheaths, where the solar wind slows down and heats up, control a significant part of the magnetosphere's dynamics (Formisano et al., 1973; S. Y. Huang, 2022; Huang, Wang, et al., 2020; Huang et al., 2014; Sahraoui et al., 2006), reason for which turbulence (and other processes) have been studied in those environments. In the case of the Earth's magnetosheath, previous studies showed that the spectra with the Kolmogorov scaling account only for a small fraction (∼17%) of the total analyzed spectra (Huang et al., 2017). This proportion is 15% in Mercury's magnetosheath (Huang, Wang, et al., 2020), while Hadid et al. (2015) found no evidence of the Kolmogorov inertial range within the data sets they analyzed although steeper spectra than f^{-1} and intermittent (multi-fractal) fluctuations were evidenced downstream of the quasi-parallel shock. In Jupiter's magnetosheath, Bandyopadhyay et al. (2021) have presented a case study where ion density and velocity spectra exhibit nearly a Kolmogorov scaling. Those results indicate the importance of the shock geometry in controlling the nature of the plasma turbulence. This role can be manifested either by "resetting" some properties of the turbulence preexisting in the solar wind or by controlling the strength of the nonlinear effects thus leading to the reformation of fully developed turbulent state far away from the shock (Bandyopadhyay et al., 2021; Hadid et al., 2015; Huang, Wang, et al., 2020; Huang et al., 2017).

Kolmogorov turbulence is seldom investigated within planetary magnetospheres. A possible reason is the complexity of the magnetospheric physics due to, for example, the presence of large-scale boundaries and sharp gradients, the permanent interaction with the solar wind, and the response of the magnetotail to substorms. These physical conditions make the magnetospheric plasmas unstable on various time scales that can be comparable with those of the turbulence. This can reduce the available range of scales for the turbulence to develop with respect, for instance, to the solar wind as reported in the Earth's magnetosphere (Zimbardo et al., 2010). Practically, obtaining statistical observational results (e.g., power spectra, dissipation rates) that can be reliably compared to theoretical predictions based on stationary and homogenous theories (Andrés et al., 2018; Ferrand et al., 2019; Galtier, 2008; Simon & Sahraoui, 2022) requires having long time series without the crossings of boundary. Despite these difficulties, deep physical insight was obtained from previous observational studies in the terrestrial magnetosphere (Vörös et al., 2004, 2007; Zimbardo et al., 2010). Here, we extend those efforts to the Saturn's magnetosphere using the measurements from the Cassini spacecraft.

2. Data and Results

We used the 6 years of data from 2004 to 2009 when Cassini traveled in the Saturn's magnetosphere. The magnetic field data were provided by the MAG instrument of the Cassini spacecraft (Dougherty et al., 2004). The sampling frequency of MAG ranges from 4 to 32 Hz. The magnetic field data is down-sampled to 2 Hz to get the spectra in the frequency range $[10^{-4}, 1]$ Hz. The electron measurements are supplied by the Cassini Plasma Spectrometer (CAPS) (Young et al., 2004).

We calculated PSDs of the magnetic field and electron density using the Morlet wavelet transform. To convert the frequencies measured onboard the spacecraft into wavenumbers the Taylor's frozen-in approximation is applied, that is, $w = \boldsymbol{k}.\boldsymbol{V}_{\text{flow}}$. In Saturn's magnetosphere, the Alfvén velocities V_A is of the same order than $\boldsymbol{V}_{\text{flow}}$ (Thomsen et al., 2010), implying that Taylor's hypothesis may not be applicable in all circumstances. Under some assumptions it still can hold, such as in the highly oblique Kinetic Alfvén Waves (KAWs) (Howes et al., 2014; Huang & Sahraoui, 2019; Klein et al., 2014; Sahraoui et al., 2006, 2009; von Papen et al., 2014).

In solar wind, the spectral breaks separating the MHD scales and kinetic scales may correspond to three ion characteristic scales, namely the ion Larmor radius $\rho_{\text{i}} = V_{th\perp}/\Omega_i$, the ion initial length $d_{\text{i}} = V_A/\Omega_i$, and the ion cyclotron frequency $f_{\text{ci}} = \Omega_i/2\pi$ (Kiyani et al., 2015). Here, $\Omega_i = eB_0/m_i$, $V_{\text{th}\perp} = (2k_{\text{B}}T_{i\perp}/m_i)^{1/2}$ is the perpendicular thermal speed, $V_A = B_0/(\mu_0 n_i m_i)^{1/2}$. The two first scales correspond when Taylor-shifted to the frequencies $f_{\rho i} = V_{\text{flow}}/2\pi\rho_{\text{i}}$ and $f_{\text{di}} = V_{\text{flow}}/2\pi d_i$, respectively. Two ion species (H^+, water group ions W^+) are reported in the Saturn's magnetosphere (von Papen et al., 2014), which we consider in this study. We further assume a mean ion mass of $m = 18$ amu (H_2O^+) for W^+ and note $f_{\rho,w}, f_{d,w}$ and $f_{c,w}$ their characteristic scales as defined above.

Figure 1 displays two examples of Kolmogorov turbulence events in Saturn's magnetosphere. The blue curve in Figure 1a is the Cassini trajectory during the dayside event observed between 03:00 and 09:00 UT on 11 October 2005 at Saturn local time of [10.3, 10.9], and the orange curve is the trajectory during the nightside event observed

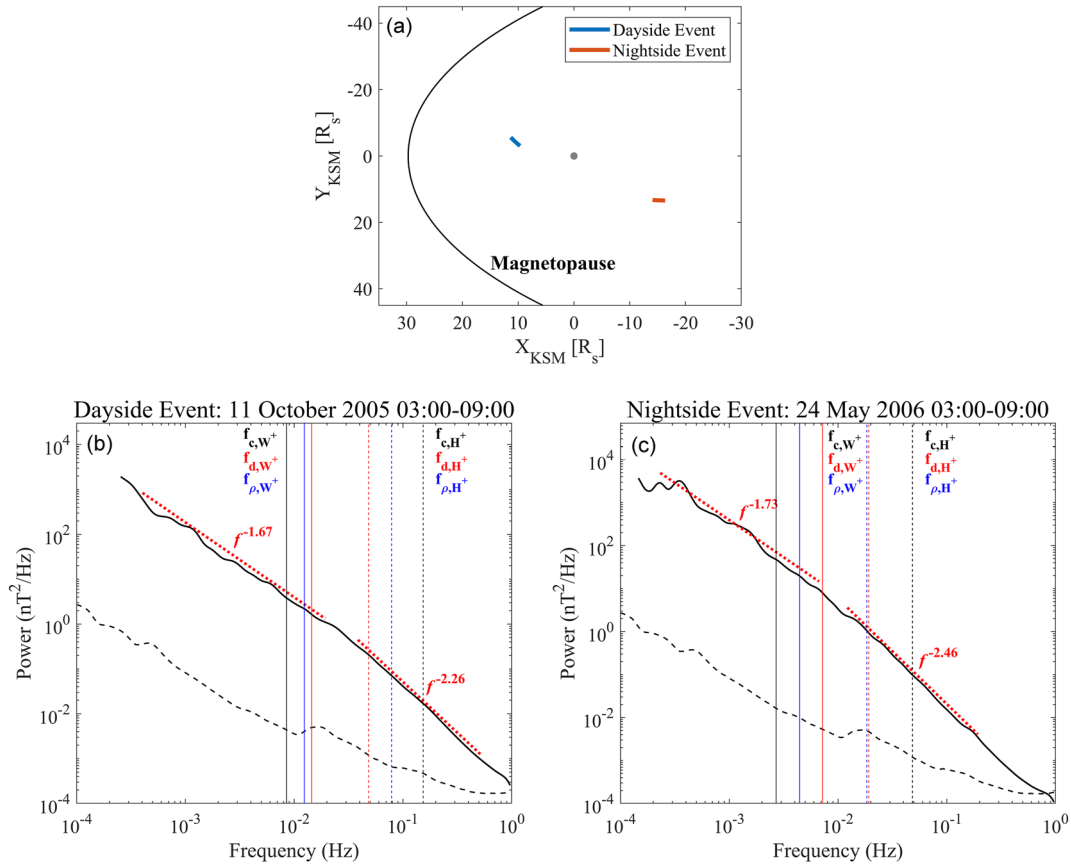

Figure 1. Two examples of Kolmogorov turbulence observed in Saturn's magnetosphere. (a) Cassini's trajectories of dayside event and nightside event; (b, c) The power spectral densities of the magnetic field measured in the dayside magnetosphere and the magnetotail, respectively. The dashed curves in (b, c) are magnetic field spectra measured in the solar wind, considered here to represent the upper bound of the sensitivity floor of MAG. The solid vertical lines represent the characteristic scales of ion and the dotted vertical lines represent the characteristic scales of water group ion.

between 03:00 and 09:00 on 24 May 2006 at Saturn local time of [21.2, 21.5]. The position of the magnetopause is calculated under 0.005 nPa of the solar wind pressure based on the model of Kanani et al. (2010). The background plasma parameters are given as $d_i \sim 233$ km, $\rho_i \sim 143$ km, $d_w \sim 775$ km, $\rho_w \sim 907$ km for the dayside event, and given as $d_i \sim 715$ km, $\rho_i \sim 747$ km, $d_w \sim 1924$ km, $\rho_w \sim 3156$ km for the nightside event. The magnetic-field fluctuation level given by $\delta B/\langle B\rangle$ is found to be 0.054 and 0.123 in the two events, indicating a weak amplitude fluctuation with respect to the background field. Here, δB is the root mean square of $(B(t)-\langle B\rangle)$, where $\langle B\rangle$ is a moving average of $B(t)$ and the smoothing time is set as 2 hr Figures 1b and 1c show the magnetic field spectra of both events. Both spectra display nearly power-law behavior in two frequency bands separated by a break. A linear fitting in logarithmic scale of these two ranges reveals spectral slopes close to $-5/3$ at low frequencies and to $-7/3$ at the higher ones. This observation agrees with theoretical prediction of the $k^{-5/3}$ power law in the inertial range of scales, which is routinely observed in solar wind turbulence (e.g., Goldstein et al., 1995; Leamon et al., 1998; Sahraoui et al., 2010, 2013).

While spectral breaks in solar wind turbulence are frequently compared to proton characteristic scales (considering the small fraction of the heavier ions that constitute the plasma, Chen et al., 2014), here they occur at scales ranging between $f_{c,w}$ and $f_{c,H}$. This may be explained to the large proportion of water-group ions in Saturn's magnetosphere (von Papen et al., 2014). Their large scales (compared with the proton ones) yield a spectral break at lower frequencies, which renders this multi-species (heavy ion, proton and electron) plasma turbulence more complex than the classical two fluid (proton and electron) one.

The auto-correlation function of magnetic fluctuations can be seen as a measure of the "memory" that a signal has of itself. Matthaeus and Goldstein (1982b) suggested that the correlation function can be fitted in exponential

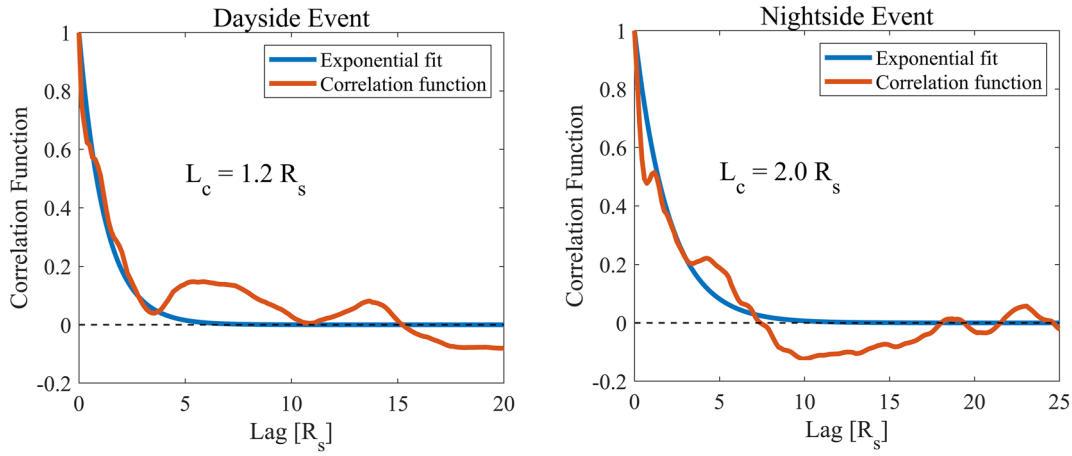

Figure 2. Magnetic field correlation functions as a function of spatial scale in units of Saturn's radii (Rs) for the dayside event and the nightside event. The exponential fit yields the correlation length of $L_c \approx 1.2$ Rs for the dayside event and $L_c \approx 2.0$ Rs for the nightside event. The horizontal dashed lines mark "0" for the correlation functions.

form when the data satisfy stationarity and ergodicity. Here, we calculated the correlation functions (shown in Figure 2) for the dayside and nightside events. The correlation is defined as $R(l) = <\delta B(x).\ \delta B(x + l)>$, where l is a spatial lag that be related to the time lag τ by $l = \tau\ V_{flow}$ assuming the Taylor hypothesis. The correlation length (L_c) is estimated as the scale where the correlation function $R(l)$ reaches the value of $R(0)$/e. Here, the correlation length is estimated to 1.2 Rs (Rs ~ 60,268 km, radius of Saturn) and 2.0 Rs for the dayside and nightside events respectively; the blue curves in Figure 2 indicate the exponential fits $e^{-l/Lc}$. The correlation length can be compared with the ion characteristic scale to estimate the effective Reynolds number R_e (Bandyopadhyay, Matthaeus, Chasapis, et al., 2020; Bandyopadhyay, Matthaeus, Parashar, Chhiber, et al., 2020; Bandyopadhyay, Matthaeus, Parashar, Yang et al., 2020; Matthaeus et al., 2005). We found, $L_c/\rho_i \sim 504$, $L_c/\rho_w \sim 80$, $R_e \sim (L_c/\rho_i)^{4/3} \sim 4011$ for the dayside event and $L_c/\rho_i \sim 161$, $L_c/\rho_w \sim 38$, $R_e \sim 878$ for the nightside event. The broad separation of scales (2–3 decades) allows the turbulence cascade to proceed from the scales $\sim L_c$ to scales $\sim \rho_i$, where kinetic effects become important.

We calculated the electron density spectra (shown in Figure 3) based on a 24-hr interval from 12:00 on 10 October 2005 to 12:00 on 11 October 2005. The electron spectrum shows a nearly power-law behavior in the frequency space between 5×10^{-5} and 10^{-3} Hz. Using a least-square straight-line fitting in log-log space for this range, the spectral index for the density spectrum is −1.76, which is close to Kolmogorov scaling of $\sim f^{-5/3}$. The −5/3 inertial-range spectrum of number density fluctuation suggests nearly incompressible magnetohydrodynamics turbulence (Bandyopadhyay et al., 2021). The two peaks observed within the band $[10^{-3}, 10^{-2}]$ Hz of the electron density spectrum, which are also measured in the solar wind spectra (the dashed curves in Figure 3a), are not real fluctuation. This may be due to the periodic change of the field of view orientation of the CAPS instrument (Young et al., 2004).

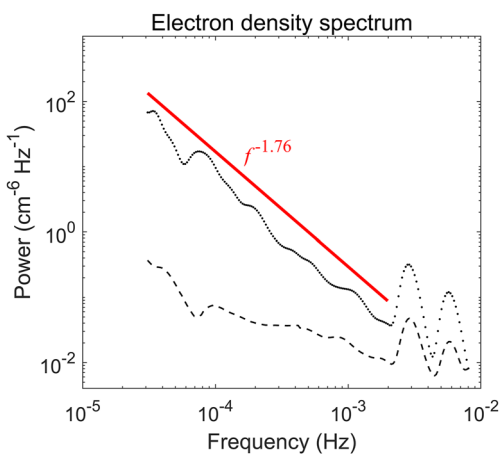

Figure 3. Power spectral densities of electron density measured in Saturn's magnetosphere from 12:00 on 10 October 2005 to 12:00 on 11 October 2005. The dashed curve is electron density spectrum measured in the solar wind, considered here to represent the upper bound of the sensitivity floor of electron measurements.

To obtain a global picture as to how turbulence properties behave in the Saturn's magnetosphere, we carried out a statistical study of the magnetic power spectra calculated every 6 hr. The Kolmogorov scaling −5/3 (~−1.66) in the inertial range is the characteristic of Kolmogorov event. Considering a 10% of confidence interval, the magnetic field spectra with spectral indexes in $[-1.66 - 0.16, -1.66 + 0.16] = [-1.82, -1.5]$ will be classified as Kolmogorov-like events. Based on 6 years of Cassini data, 1687 Kolmogorov events have been successfully selected. The locations of all Kolmogorov events are projected onto the Kronocentric Solar Magnetospheric (KSM) coordinates in Figure 4. Figures 4a and 4b show the number of the events in

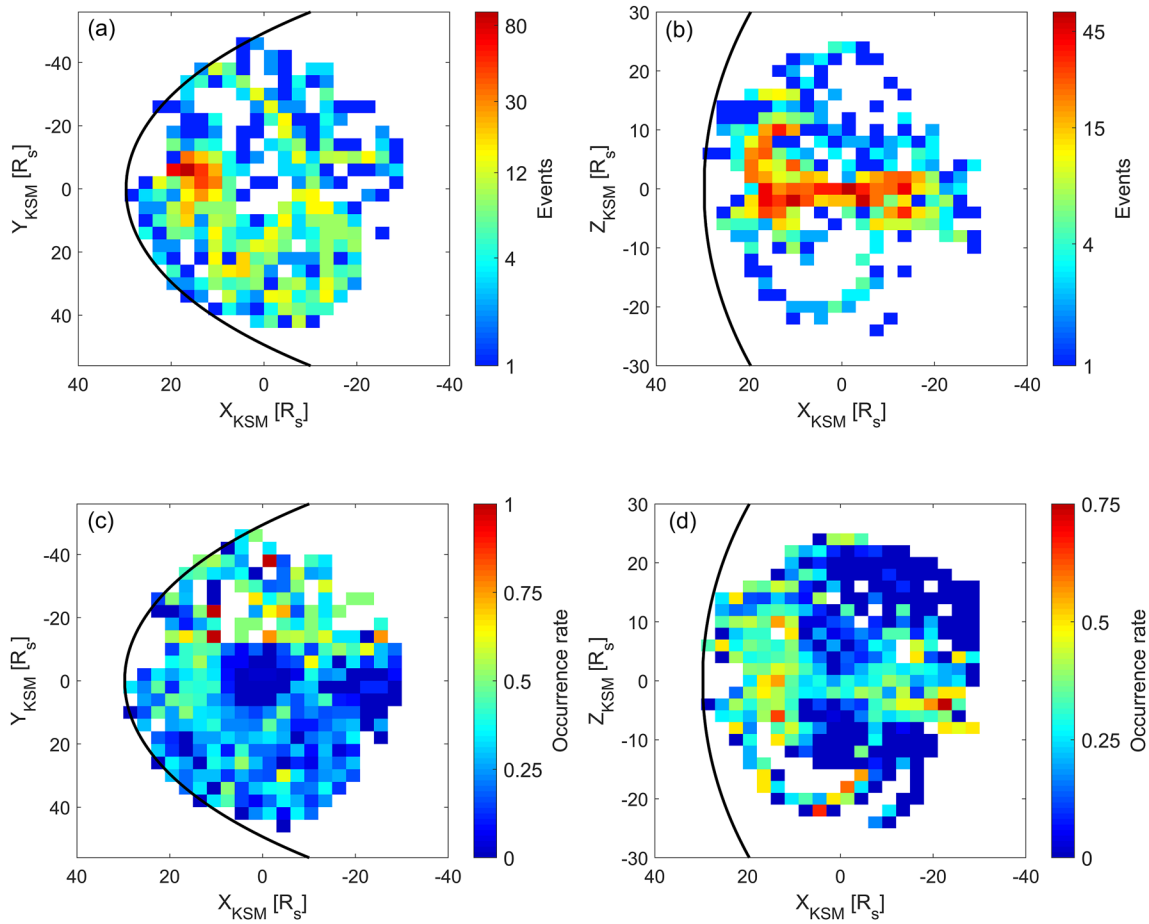

Figure 4. The spatial distribution of Kolmogorov turbulence in Saturn's magnetosphere. (a, b) The number of Kolmogorov turbulence events in the X-Y plane (a) and X-Z plane (b) of Kronocentric Solar Magnetospheric (KSM) coordinates. (c, d) The occurrence rate in the X-Y plane (c) and X-Z plane (d) of KSM coordinates. The black curves represent the magnetopause under the solar wind pressure of 0.005 nPa.

the *X-Y* plane and *X-Z* plane of the KSM coordinates. In the *X-Y* plane, one can see that turbulence is seemingly fully developed within the whole magnetosphere, not only on the tail-side but also on the dayside, dawn-side and dusk-side. Compared with other bins, the region of $X \sim [15, 18]$ Rs, $Y \sim [-8, -4]$ Rs has the largest number of the Kolmogorov events (see below about the possible bias due to Cassini orbit sampling). In the *X-Z* plane, most Kolmogorov spectra are concentrated in $Z \sim [-10, 10]$ Rs, which is the region of Saturn's magnetodisc current sheet (e.g., Arridge et al., 2008). On the dayside magnetosphere, a considerable number of the Kolmogorov events is measured close to the magnetopause, and the location of these events extends even to $Z = \pm 20$ Rs. Both observations suggest the potential role played by the large scale magnetosheric currents (the magnetodisc and the magnetopause) in the generation and evolution of the magnetospheric turbulence.

Considering the orbit bias of Cassini, the occurrence rate of Kolmogorov turbulence is presented in Figures 4c and 4d. The occurrence rate is defined by the ratio between the number of Kolmogorov turbulence events and the whole number of 6-hr intervals in each bin. The occurrence rate of the Kolmogorov events is 26.11% for the whole magnetosphere. This value is even higher (up to 30.37%) for the outer magnetosphere ($R_{xy} > 10$ Rs) and up to 35.61% for the current sheet region ($Z \sim [-10, 10]$ Rs). These values in Saturn's magnetosphere are much larger than the occurrence rate found in the Earth's magnetosheath (17%, Huang et al., 2017) and Mercury's magnetosheath (15%, Huang, Wang, et al., 2020). Comparing the Reynolds number in Saturn's magnetosphere to that in Earth's magnetosheath may provide some explanations for this result. Through fitting the correlation function, the correlation length (L_c) is estimated as the scale where the correlation function $R(l)$ reaches the value of $R(0)$/e. Then the Reynolds number R_e is calculated by $(L_c/\rho_i)^{4/3}$. According to the results presented by Huang et al. (2017), the Reynolds number for most events in Earth's magnetosheath ranges from 12 to 251. The Reynolds

numbers calculated for the Kolmogorov-like event in the Saturn's magnetosphere range from around 1,000 to 4,000, which is much larger than that in the Earth's magnetosheath. Moreover, the occurrence rate gets close to 0 when the distance from the Saturn is less than 10 Rs in the *X-Y* plane, indicating that Kolmogorov turbulence does not develop in the inner magnetosphere. The occurrence rate of Kolmogorov turbulence in the dawn-side is higher than in the dusk-side. This dawn-dusk asymmetry provides some lead about the origin of Kolmogorov turbulence, as discussed below.

Solar wind turbulence at MHD scales is thought be dominated by incompressible Alfvénic fluctuations characterized by $\delta B_\perp >> \delta B_{||}$ (e.g., Goldstein et al., 1995; Sahraoui et al., 2010) while the compressible component ($\delta B_{||} > \delta B_\perp$)has a weaker contribution (Howes et al., 2014; Klein et al., 2014). Here, to identify the nature of turbulent fluctuations in the Kolmogorov-like events, we use the magnetic compressibility $C_{||}$ given by the ratio between the PSDs of the parallel magnetic field component and the magnetic field magnitude, $C_{||}(f) = |\delta B_{||}(f)|^2/(|\delta B_{||}(f)|^2+|\delta B_\perp(f)|^2)$. Referring to the theoretical magnetic compressibility calculated from the linear solutions of the Vlasov–Maxwell using the WHAMP code (Ronnmark, 1982), different plasma modes have different $C_{||}$ (Hadid et al., 2015; Huang, Wang, et al., 2020; Huang et al., 2017). For turbulence dominated by incompressible Alfvénic fluctuations $C_{||}$ is low (∼0) at MHD scales but increases to nearly 1/3 at kinetic scales (power isotropization, Kiyani et al., 2015). For compressible turbulence (fast or slow magnetosonic-like modes) $C_{||}$, although is β—dependent, is generally larger than 1/3. To suppress the varying background field in the magnetosphere, the parallel component of fluctuations is calculated by $\delta B_{||}^2 = \delta|B|^2$ (e.g., Chen et al., 2012), while the perpendicular one is obtained from $\delta B_\perp^2 = \delta B_r^2 + \delta B_\theta^2 + \delta B_\varphi^2 - \delta B_{||}^2$. Here, $\delta|B|$ is the symbol in the frequency domain, which is obtained by the wavelet transform of $|B|$. Our statistical results show that 1147 Kolmogorov-like events have magnetic compressibility smaller than 1/3 at MHD scales accounting for 67.99% of the total. This result agrees with the assumption promoted by von Papen et al. (2014) that most fluctuations have $\delta B_\perp^2 > \delta B_{||}^2$ in the Saturn's magnetosphere. Among them, 753 events have rising profiles that are characteristic of Alfvénic turbulence, accounting for 44.64% of the total events. Only 117 events (6.94% of the total) are found to have a high magnetic compressibility ($C_{||} > 1/3$) from 10^{-3} Hz–0.5 Hz, and identified as magnetosonic-like turbulence. Figures 5a and 5d show the profiles of the magnetic compressibility as function of the frequency for the Kolmogorov events, which reflect the magnetosonic (Figure 5a) versus the Alfvénic (Figure 5b) nature of the fluctuations. Their respective spatial distributions in the Saturn's magnetosphere are also shown (Figures 5b and 5c and Figures 5e and 5f). Alfvénic turbulence is seldom observable within 10 Rs of *X-Y* plane. In contrast, compressible (magnetosonic-like) turbulence tends to be distributed closer to Saturn in *X-Y* plane and seem to be localized at $Z \sim [-5, 5]$ Rs (although the occurrence rate may partly balance this claim), which is the region of the Saturn's magnetodisc current sheet. Malara et al. (1996) suggested that the interaction between Alfvénic fluctuations and the current sheet can generate the compressive fluctuations. Moreover, there are 423 events whose spectra show $\delta B_\perp > \delta B_{||}$ at some frequencies and $\delta B_{||} > \delta B_\perp$ at other frequencies.

We also analyzed the dependence of the number of Kolmogorov events on the varied confidence interval. Based on a 15% confidence interval (spectral index ∼[−1.90, −1.42]), the number of Kolmogorov events is 2404. For confidence intervals of 10% ([−1.82, −1.50]), 7% ([−1.78, −1.54]), 5% ([−1.75, −1.57]), the corresponding numbers of Kolmogorov events are 1687, 1277, and 959, respectively. However, the selection of the confidence interval does not affect the conclusions drawn in present study.

3. Discussions and Conclusions

Saturn is a giant gas planet with a relatively large magnetosphere. The magnetosphere can extend up to 20 Rs (depending on solar wind pressure) in the subsolar direction and up to 60 Rs at the tail-side (Arridge et al., 2008). The vast size of the magnetosphere allows Cassini to collect more long-time data without boundary crossing. This is reflected in Figure 1 where the observed spectra range from quite a low frequency edge of 10^{-4} Hz–∼1 Hz. In present study, we analyze the occurrence and distribution of the magnetic field spectra with Kolmogorov scaling in the inertial range based on the large statistical samples. Our result shows the extensive and numerous distributions of Kolmogorov-like events observed at all local times of Saturn's magnetosphere, including the noon-side, dusk-side, dawn-side, and night-side. The occurrence rate of the Kolmogorov events in Saturn's magnetosphere is even much larger than the occurrence rate found in the planetary magnetosheath which are known for their strong turbulent environment.

The Kolmogorov scaling in the inertial range of scales is characteristic of fully developed turbulence (Kolmogorov, 1941) and indicates the presence of a scale-invariant energy cascade through the inertial range of scales (Verma et al., 1995). Our statistical result reveals a high occurrence rate of Kolmogorov-like turbulence in

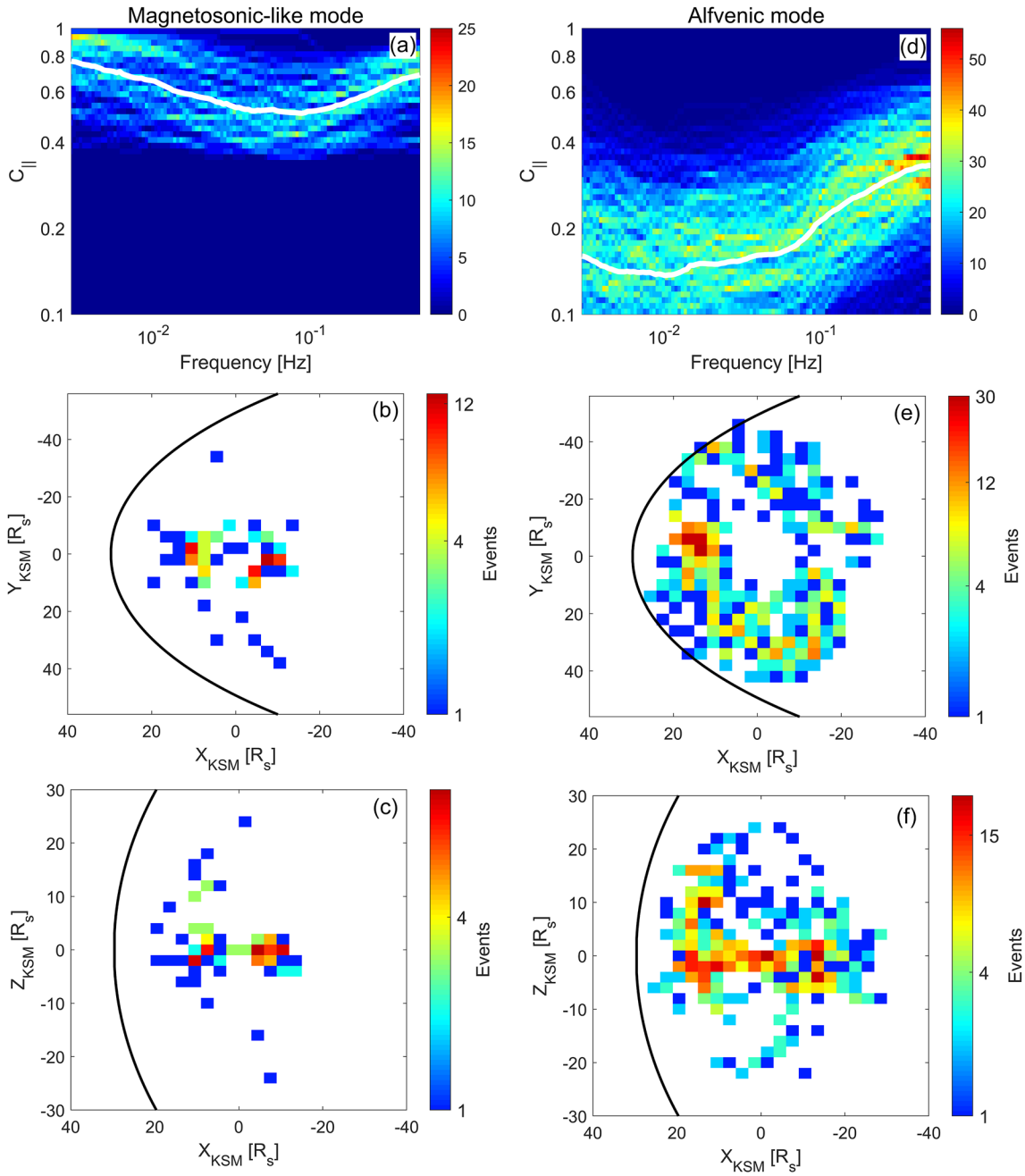

Figure 5. Profile of the of magnetic compressibility and the spatial distribution for magnetosonic-like mode (117 events) Kolmogorov turbulence events (a–c), and Alfvénic mode (753 events) Kolmogorov turbulence events (d–f). In panel (a and d), the colors represent the number of events in each bin and the white curves are median values.

Saturn's magnetosphere, which indicates that the plasma environment of Saturn's magnetosphere may be conducive to reaching a fully developed turbulence state. In this work, we calculated the correlation length and the Reynolds number for the Kolmogorov-like event. The Reynolds numbers calculated in the Saturn's magnetosphere range from around 1,000 to 4000, which are generally larger than that calculated in Earth's magnetosheath. Large Reynolds number broadens the available scales of the observed spectra, allowing a broad scale separation favorable to fully developing turbulence.

Based on Cassini observations on Saturn (Hadid et al., 2015), Cluster observations on Earth (Huang et al., 2017) and Messenger observations on Mercury (Huang, Wang, et al., 2020), a common phenomenon is that the magnetic

spectra measured near the bow shock show a direct transition from the energy containing scales characterized by the *1/f* spectrum to the ion kinetic scales $\sim f^{-2.8}$ without forming the Kolmogorov inertial range $\sim f^{-5/3}$; however, in the flanks region located far away from the bow shock, the spectra steepen from −1 to −5/3 at MHD scales. A possible explanation is that the interaction with the bow shock "destroys" pre-existing correlations in the solar wind leading to random-like (uncorrelated) fluctuations (Huang et al., 2017). Downstream in the magnetosheath, correlations between the fluctuations reappear due to nonlinear effects, after a period of time that can be estimated as $T_c \sim L_c/V_{\text{flow}}$, also called "eddy turn-over time." For the dayside and the nightside events (shown in Figure 1) in Saturn's magnetosphere, the correlation time T_c is estimated to 0.61 and 0.52 hr, respectively. Considering the plasma environment of Saturn's magnetosphere, the plasma is generally found to be sub-corotating and has a rotation period of ∼10 hr due to the rapid rotation of Saturn. Assuming that the magnetospheric plasma survives for the time comparable to the rotation period, the turbulence plasmas have time to develop for several correlation times, which supports the existence of an extended inertial range. Moreover, the global plasma rotation also contributes to the azimuthal diffusion of turbulence. This diffusion process in azimuthal direction provides a possible explanation for our statistical result that the Kolmogorov turbulence can be observed at every local time.

Kelvin-Helmholtz instability is a large-scale velocity shear-driven instability that has been frequently reported to occur on the flanks of planetary magnetopauses (e.g., Delamere et al., 2013; Hasegawa et al., 2004). Both simulations and observations have shown that Kelvin-Helmholtz instability can generate MHD turbulence with Kolmogorov scaling (Hwang et al., 2011; Matsumoto & Hoshino, 2004; Stawarz et al., 2016). At Saturn's magnetopause, Voyager 1 first observed the Kelvin-Helmholtz instability (Lepping et al., 1981). Galopeau et al. (1995) showed the importance of the local time effect on the Kelvin-Helmholtz instability at Saturn's magnetopause and reported that the different flow shear conditions excite the Kelvin-Helmholtz instability more in the dawn-side than in the dusk-side. Our statistical results revealed a similar asymmetry in the dayside Kolmogorov turbulence events near the magnetopause. The occurrence rate of the Kolmogorov spectra in the dawn-side is higher than that in the dusk-side. This result points toward the role of the Kelvin-Helmholtz instability in generating Kolmogorov turbulence in Saturn's magnetosphere.

Data Availability Statement

We thank the entire Cassini team and instrument leads for data access and support. Cassini data is publicly available from The Planetary Plasma Interactions (PPI) Node of the Planetary Data System (PDS) at https://pds-ppi.igpp.ucla.edu/search/?t=Saturn&sc=Cassini&facet=SPACECRAFT_NAME&depth=1. The magnetic field data were provided by the MAG instrument of the Cassini spacecraft, and the DOI for MAG is https://doi.org/10.17189/1521151. The magnetic field data used in this paper were downloaded at https://pds-ppi.igpp.ucla.edu/search/view/?f=yes&id=pds://PPI/CO-E_SW_J_S-MAG-3-RDR-FULL-RES-V2.0, titled as CASSINI MAGNETOMETER CALIBRATED FULL RES ARCHIVE. The magnetic field data from 2001-01-01 to 2017-09-15 was available. The plasma measurements were supplied by the Cassini Plasma Spectrometer (CAPS), and the DOI for CAPS is https://doi.org/10.17189/1519593. The electron moments data which include electron density and temperature data were downloaded at https://pds-ppi.igpp.ucla.edu/search/view/?f=yes&id=pds://PPI/cassini-caps-derived/data-ele-mom, titled as Cassini-Huygens Plasma Spectrometer (CAPS) Derived Electron Moments Data Collection. The ion moments data which include ion density, velocity, and temperature data were downloaded at https://pds-ppi.igpp.ucla.edu/search/view/?f=yes&id=pds://PPI/cassini-caps-derived/data-ion-moments, titled as Cassini-Huygens Cassini Plasma Spectrometer (CAPS) Derived Ion Moments Data Collection. The plasma measurements from 1999-01-04 to 2012-06-02 are available.

Acknowledgments
This work was supported by the National Natural Science Foundation of China (42074196, 41925018) and the National Youth Talent Support Program, and the project supported by Special Fund of Hubei Luojia laboratory.

References

Andrés, N., Galtier, S., & Sahraoui, F. (2018). Exact law for homogeneous compressible hall magnetohydrodynamics turbulence. *Physical Review*, *97*(1), 013204. https://doi.org/10.1103/physreve.97.013204

Andrés, N., Romanelli, N., Hadid, L. Z., Sahraoui, F., DiBraccio, G., & Halekas, J. (2020). Solar wind turbulence around Mars: Relation between the energy cascade rate and the proton cyclotron waves activity. *The Astrophysical Journal*, *902*(2), 134. https://doi.org/10.3847/1538-4357/abb5a7

Arridge, C. S., Russell, C. T., Khurana, K. K., Achilleos, N., Cowley, S. W. H., Dougherty, M. K., et al. (2008). Saturn's magnetodisc current sheet. *Journal of Geophysical Research*, *113*(A2), A04214. https://doi.org/10.1029/2007JA012538

Bale, S. D., Kellogg, P. J., Mozer, F. S., Horbury, T. S., & Reme, H. (2005). Measurement of the electric fluctuation spectrum of magnetohydrodynamic turbulence. *Physical Review Letters*, *94*(21), 215002. https://doi.org/10.1103/PhysRevLett.94.215002

Bandyopadhyay, R., Chasapis, A., Chhiber, R., Parashar, T. N., Maruca, B. A., Matthaeus, W. H., et al. (2018). Solar wind turbulence studies using MMS fast plasma investigation data. *The Astrophysical Journal*, *866*(2), 81. https://doi.org/10.3847/15384357/aade93

Bandyopadhyay, R., Chasapis, A., Chhiber, R., Parashar, T. N., Matthaeus, W. H., Shay, M. A., et al. (2018). Incompressive energy transfer in the Earth's magnetosheath: Magnetospheric multiscale observations. *The Astrophysical Journal*, *866*(2), 106. https://doi.org/10.3847/1538-4357/aade04

Bandyopadhyay, R., Matthaeus, W. H., Chasapis, A., Russell, C. T., Strangeway, R. J., Torbert, R. B., et al. (2020). Direct measurement of the solar-wind Taylor microscale using MMS turbulence campaign data. *The Astrophysical Journal*, *899*(1), 63. https://doi.org/10.3847/1538-4357/ab9ebe

Bandyopadhyay, R., Matthaeus, W. H., Parashar, T. N., Chhiber, R., Ruffolo, D., Goldstein, M. L., et al. (2020). Observations of energetic-particle population enhancements along intermittent structures near the Sun from the Parker Solar Probe. *The Astrophysical Journal - Supplement Series*, *246*(2), 61. https://doi.org/10.3847/1538-4365/ab6220

Bandyopadhyay, R., Matthaeus, W. H., Parashar, T. N., Yang, Y., Chasapis, A., Giles, B. L., et al. (2020). Statistics of kinetic dissipation in the Earth's magnetosheath: MMS observations. *Physical Review Letters*, *124*(25), 255101. https://doi.org/10.1103/PhysRevLett.124.255101

Bandyopadhyay, R., McComas, D. J., Szalay, J. R., Allegrini, F., Bolton, S. J., Ebert, R. W., et al. (2021). Observation of Kolmogorov turbulence in the Jovian magnetosheath from JADE data. *Geophysical Research Letters*, *48*(15), e2021GL095006. https://doi.org/10.1029/2021gl095006

Bavassano, B., Dobrowolny, M., Mariani, F., & Ness, N. F. (1982). Radial evolution of power spectra of interplanetary Alfvénic turbulence. *Journal of Geophysical Research*, *87*(A5), 3617–3622. https://doi.org/10.1029/ja087ia05p03617

Bruno, R., & Carbone, V. (2013). The solar wind as a turbulence laboratory. *Living Reviews in Solar Physics*, *10*(1), 1–208. https://doi.org/10.12942/lrsp-2013-2

Chandran, B. D. (2018). Parametric instability, inverse cascade and the range of solar-wind turbulence. *Journal of Plasma Physics*, *84*(1), 905840106. https://doi.org/10.1017/s0022377818000016

Chen, C. H. K., Leung, L., Boldyrev, S., Maruca, B. A., & Bale, S. D. (2014). Ion-scale spectral break of solar wind turbulence at high and low beta. *Geophysical Research Letters*, *41*(22), 8081–8088. https://doi.org/10.1002/2014gl062009

Chen, C. H. K., Mallet, A., Schekochihin, A. A., Horbury, T. S., Wicks, R. T., & Bale, S. D. (2012). Three-dimensional structure of solar wind turbulence. *The Astrophysical Journal*, *758*(2), 120. https://doi.org/10.1088/0004-637x/758/2/120

Coleman, P. J., Jr. (1968). Turbulence, viscosity, and dissipation in the solar-wind plasma. *The Astrophysical Journal*, *153*, 371. https://doi.org/10.1086/149674

Delamere, P. A., Wilson, R. J., Eriksson, S., & Bagenal, F. (2013). Magnetic signatures of Kelvin-Helmholtz vortices on Saturn's magnetopause: Global survey. *Journal of Geophysical Research: Space Physics*, *118*(1), 393–404. https://doi.org/10.1029/2012JA018197

Dougherty, M. K., Kellock, S., Southwood, D. J., Balogh, A., Smith, E. J., Tsurutani, B. T., et al. (2004). The Cassini magnetic field investigation. *Space Science Reviews*, *114*(1–4), 331–383. https://doi.org/10.1007/s11214-004-1432-2

Ferrand, R., Galtier, S., Sahraoui, F., Meyrand, R., Andrés, N., & Banerjee, S. (2019). On exact laws in incompressible hall magnetohydrodynamic turbulence. *The Astrophysical Journal*, *881*(1), 50. https://doi.org/10.3847/1538-4357/ab2be9

Formisano, V., Moreno, G., Palmiotto, F., & Hedgecock, P. C. (1973). Solar wind interaction with the Earth's magnetic field: 1, Magnetosheath. *Journal of Geophysical Research*, *78*(19), 3714–3730. https://doi.org/10.1029/ja078i019p03714

Galopeau, P. H., Zarka, P., & Le Quéau, D. (1995). Source location of Saturn's kilometric radiation: The Kelvin-Helmholtz instability hypothesis. *Journal of Geophysical Research*, *100*(E12), 26397–26410. https://doi.org/10.1029/95je02132

Galtier, S. (2008). von Kármán–Howarth equations for hall magnetohydrodynamic flows. *Physical Review*, *77*(1), 015302. https://doi.org/10.1103/physreve.77.015302

Goldstein, M. L., Roberts, D. A., & Fitch, C. A. (1994). Properties of the fluctuating magnetic helicity in the inertial and dissipation ranges of solar wind turbulence. *Journal of Geophysical Research*, *99*(A6), 11519–11538. https://doi.org/10.1029/94ja00789

Goldstein, M. L., Roberts, D. A., & Matthaeus, W. H. (1995). Magnetohydrodynamic turbulence in the solar wind. *Annual Review of Astronomy and Astrophysics*, *33*(1), 283–325. https://doi.org/10.1146/annurev.aa.33.090195.001435

Hadid, L. Z., Sahraoui, F., Kiyani, K. H., Retinò, A., Modolo, R., Canu, P., et al. (2015). Nature of the MHD and kinetic scale turbulence in the magnetosheath of Saturn: Cassini observations. *The Astrophysical Journal Letters*, *813*(2), L29. https://doi.org/10.1088/2041-8205/813/2/l29

Hasegawa, H., Fujimoto, M., Phan, T.-D., Rème, H., Balogh, A., Dunlop, M. W., et al. (2004). Transport of solar wind into Earth's magnetosphere through rolled-up Kelvin-Helmholtz vortices. *Nature*, *430*(7001), 755–758. https://doi.org/10.1038/nature02799

He, J. S., Marsch, E., Tu, C. Y., Zong, Q. G., Yao, S., & Tian, H. (2011). Two-dimensional correlation functions for density and magnetic field fluctuations in magnetosheath turbulence measured by the Cluster spacecraft. *Journal of Geophysical Research*, *116*(A6), A06207. https://doi.org/10.1029/2010ja015974

Horbury, T. S., Forman, M., & Oughton, S. (2008). Anisotropic scaling of magnetohydrodynamic turbulence. *Physical Review Letters*, *101*(17), 175005. https://doi.org/10.1103/PhysRevLett.101.175005

Howes, G. G., Klein, K. G., & TenBarge, J. M. (2014). Validity of the Taylor hypothesis for linear kinetic waves in the weakly collisional solar wind. *The Astrophysical Journal*, *789*(2), 106. https://doi.org/10.1088/0004-637x/789/2/106

Howes, G. G., TenBarge, J. M., & Dorland, W. (2011). A weakened cascade model for turbulence in astrophysical plasmas. *Physics of Plasmas*, *18*(10), 102305. https://doi.org/10.1063/1.3646400

Huang, S., Sahraoui, F., Deng, X., He, J., Yuan, Z., Zhou, M., et al. (2014). Kinetic turbulence in the terrestrial magnetosheath: Cluster observations. *The Astrophysical Journal Letters*, *789*(2), L28. https://doi.org/10.1088/2041-8205/789/2/l28

Huang, S. Y. (2022). The Earth's magnetosheath: Structures, waves and turbulence. *Reviews of Geophysics and Planetary Physics*, *53*(5), 517–531. (in Chinese). https://doi.org/10.19975/j.dqyxx.2022-014

Huang, S. Y., Hadid, L. Z., Sahraoui, F., Yuan, Z. G., & Deng, X. H. (2017). On the existence of the Kolmogorov inertial range in the terrestrial magnetosheath turbulence. *The Astrophysical Journal Letters*, *836*(1), L10. https://doi.org/10.3847/2041-8213/836/1/l10

Huang, S. Y., & Sahraoui, F. (2019). Testing of the Taylor frozen-in-flow hypothesis at electron scales in the solar wind turbulence. *The Astrophysical Journal*, *876*(2), 138. https://doi.org/10.3847/1538-4357/ab17d3

Huang, S. Y., Sahraoui, F., Andrés, N., Hadid, L. Z., Yuan, Z. G., He, J. S., et al. (2021). The Ion transition range of solar wind turbulence in the inner heliosphere: Parker solar probe observations. *The Astrophysical Journal Letters*, *909*(1), L7. https://doi.org/10.3847/2041-8213/abdaaf

Huang, S. Y., Wang, Q. Y., Sahraoui, F., Yuan, Z. G., Liu, Y. J., Deng, X. H., et al. (2020). Analysis of turbulence properties in the mercury plasma environment using MESSENGER observations. *The Astrophysical Journal*, *891*(2), 159. https://doi.org/10.3847/1538-4357/ab7349

Huang, S. Y., Xu, S. B., Zhang, J., Sahraoui, F., Andres, N., He, J. S., et al. (2022). Anisotropy of magnetic field spectra at kinetic scales of solar wind turbulence as revealed by the parker solar probe in the inner heliosphere. *The Astrophysical Journal Letters*, *929*(1), L6. https://doi.org/10.3847/2041-8213/ac5f02

Huang, S. Y., Zhang, J., Sahraoui, F., Yuan, Z. G., Deng, X. H., Jiang, K., et al. (2020). Observations of magnetic field line curvature and its role in the space plasma turbulence. *The Astrophysical Journal Letters*, *898*(1), L18. https://doi.org/10.3847/2041-8213/aba263

Huang, S. Y., Zhou, M., Sahraoui, F., Vaivads, A., Deng, X. H., André, M., et al. (2012). Observations of turbulence within reconnection jet in the presence of guide field. *Geophysical Research Letters*, *39*(11), L11104. https://doi.org/10.1029/2012GL052210

Hwang, K. J., Kuznetsova, M. M., Sahraoui, F., Goldstein, M. L., Lee, E., & Parks, G. K. (2011). Kelvin-Helmholtz waves under southward interplanetary magnetic field. *Journal of Geophysical Research*, *116*(A8), A08210. https://doi.org/10.1029/2011ja016596

Kanani, S. J., Arridge, C. S., Jones, G. H., Fazakerley, A. N., McAndrews, H. J., Sergis, N., et al. (2010). A new form of Saturn's magnetopause using a dynamic pressure balance model, based on in situ, multi-instrument Cassini measurements. *Journal of Geophysical Research*, *115*(A6), A06207. https://doi.org/10.1029/2009ja014262

Kiyani, K. H., Osman, K. T., & Chapman, S. C. (2015). Dissipation and heating in solar wind turbulence: From the macro to the micro and back again. *Philosophical Transactions of the Royal Society A: Mathematical, Physical & Engineering Sciences*, *373*(2041), 20140155. https://doi.org/10.1098/rsta.2014.0155

Klein, K. G., Howes, G. G., & TenBarge, J. M. (2014). The violation of the Taylor hypothesis in measurements of solar wind turbulence. *The Astrophysical Journal Letters*, *790*(2), L20. https://doi.org/10.1088/2041-8205/790/2/l20

Kolmogorov, A. N. (1941). Local structure of turbulence in an incompressible viscous fluid at very high Reynolds numbers. *Doklady Akademii Nauk SSSR*, *30*, 301–305. https://doi.org/10.1098/rspa.1991.0075

Leamon, R. J., Smith, C. W., Ness, N. F., Matthaeus, W. H., & Wong, H. K. (1998). Observational constraints on the dynamics of the interplanetary magnetic field dissipation range. *Journal of Geophysical Research*, *103*(A3), 4775–4787. https://doi.org/10.1029/97ja03394

Lepping, R. P., Burlaga, L. F., & Klein, L. W. (1981). Surface waves on Saturn's magnetopause. *Nature*, *292*(5825), 750–753. https://doi.org/10.1038/292750a0

Malara, F., Primavera, L., & Veltri, P. (1996). Compressive fluctuations generated by time evolution of Alfvénic perturbations in the solar wind current sheet. *Journal of Geophysical Research*, *101*(A10), 21597–21617. https://doi.org/10.1029/96ja01637

Matsumoto, Y., & Hoshino, M. (2004). Onset of turbulence induced by a Kelvin-Helmholtz vortex. *Geophysical Research Letters*, *31*(2), L02807. https://doi.org/10.1029/2003gl018195

Matteini, L., Stansby, D., Horbury, T. S., & Chen, C. H. K. (2019). The rotation angle distribution underlying magnetic field fluctuations in the 1/f range of solar wind turbulent spectra. *IL Nuovo Cimento - B*, *42*, 16. https://doi.org/10.1393/ncc/i2019-19016-y

Matthaeus, W. H., Dasso, S., Weygand, J. M., Milano, L. J., Smith, C. W., & Kivelson, M. G. (2005). Spatial correlation of solar-wind turbulence from two-point measurements. *Physical Review Letters*, *95*(23), 231101. https://doi.org/10.1103/physrevlett.95.231101

Matthaeus, W. H., & Goldstein, M. L. (1982a). Measurement of the rugged invariants of magnetohydrodynamic turbulence in the solar wind. *Journal of Geophysical Research*, *87*(A8), 6011–6028. https://doi.org/10.1029/JA087iA08p06011

Matthaeus, W. H., & Goldstein, M. L. (1982b). Stationarity of magnetohydrodynamic fluctuations in the solar wind. *Journal of Geophysical Research*, *87*(A12), 10347–10354. https://doi.org/10.1029/ja087ia12p10347

Matthaeus, W. H., & Goldstein, M. L. (1986). Low-frequency 1/f noise in the interplanetary magnetic field. *Physical Review Letters*, *57*(4), 495–498. https://doi.org/10.1103/physrevlett.57.495

Ronnmark, K. (1982). *WHAMP: Waves in homogeneous, anisotropic, multicomponent plasmas*. Kiruna Geophysical Institute.

Sahraoui, F., Belmont, G., & Rezeau, L. (2003). Hamiltonian canonical formulation of Hall-magnetohydrodynamics: Toward an application to weak turbulence theory. *Physics of Plasmas*, *10*(5), 1325–1337. https://doi.org/10.1063/1.1564086

Sahraoui, F., Belmont, G., Rezeau, L., Cornilleau-Wehrlin, N., Pinçon, J. L., & Balogh, A. (2006). Anisotropic turbulent spectra in the terrestrial magnetosheath as seen by the Cluster spacecraft. *Physical Review Letters*, *96*(7), 075002. https://doi.org/10.1103/physrevlett.96.075002

Sahraoui, F., Goldstein, M. L., Belmont, G., Canu, P., & Rezeau, L. (2010). Three-dimensional anisotropic k spectra of turbulence at subproton scales in the solar wind. *Physical Review Letters*, *105*(13), 131101. https://doi.org/10.1103/physrevlett.105.131101

Sahraoui, F., Goldstein, M. L., Robert, P., & Khotyaintsev, Y. V. (2009). Evidence of a cascade and dissipation of solar-wind turbulence at the electron gyroscale. *Physical Review Letters*, *102*(23), 231102. https://doi.org/10.1103/physrevlett.102.231102

Sahraoui, F., Hadid, L., & Huang, S. (2020). Magnetohydrodynamic and kinetic scale turbulence in the near-Earth space plasmas: A (short) biased review. *Reviews of Modern Plasma Physics*, *4*, 1–33. https://doi.org/10.1007/s41614-020-0040-2

Sahraoui, F., Huang, S. Y., Belmont, G., Goldstein, M. L., Retinò, A., Robert, P., & De Patoul, J. (2013). Scaling of the electron dissipation range of solar wind turbulence. *The Astrophysical Journal*, *777*(1), 15. https://doi.org/10.1088/0004-637x/777/1/15

Saur, J. (2021). Turbulence in the magnetospheres of the outer planets. *Frontiers in Astronomy and Space Sciences*, *56*. https://doi.org/10.3389/fspas.2021.624602

Schekochihin, A. A., Cowley, S. C., Dorland, W., Hammett, G. W., Howes, G. G., Quataert, E., & Tatsuno, T. (2009). Astrophysical gyrokinetics: Kinetic and fluid turbulent cascades in magnetized weakly collisional plasmas. *The Astrophysical Journal - Supplement Series*, *182*(1), 310–377. https://doi.org/10.1088/0067-0049/182/1/310

Simon, P., & Sahraoui, F. (2022). Exact law for compressible pressure-anisotropic magnetohydrodynamic turbulence: Toward linking energy cascade and instabilities. *Physical Review*, *105*(5), 055111. https://doi.org/10.1103/physreve.105.055111

Stawarz, J. E., Eriksson, S., Wilder, F. D., Ergun, R. E., Schwartz, S. J., Pouquet, A., et al. (2016). Observations of turbulence in a Kelvin-Helmholtz event on 8 September 2015 by the magnetospheric multiscale mission. *Journal of Geophysical Research: Space Physics*, *121*(11), 11–021. https://doi.org/10.1002/2016ja023458

Tao, C., Sahraoui, F., Fontaine, D., de Patoul, J., Chust, T., Kasahara, S., & Retinò, A. (2015). Properties of Jupiter's magnetospheric turbulence observed by the Galileo spacecraft. *Journal of Geophysical Research: Space Physics*, *120*(4), 2477–2493. https://doi.org/10.1002/2014JA020749

Thomsen, M. F., Reisenfeld, D. B., Delapp, D. M., Tokar, R. L., Young, D. T., Crary, F. J., et al. (2010). Survey of ion plasma parameters in Saturn's magnetosphere. *Journal of Geophysical Research*, *115*(A10), A10220. https://doi.org/10.1029/2010JA015267

Tu, C. Y., & Marsch, E. (1995). MHD structures, waves and turbulence in the solar wind: Observations and theories. *Space Science Reviews*, *73*(1), 1–210. https://doi.org/10.1007/bf00748891

Verma, M. K., Roberts, D. A., & Goldstein, M. L. (1995). Turbulent heating and temperature evolution in the solar wind plasma. *Journal of Geophysical Research*, *100*(A10), 19839–19850. https://doi.org/10.1029/95ja01216

von Papen, M., & Saur, J. (2016). Longitudinal and local time asymmetries of magnetospheric turbulence in Saturn's plasma sheet. *Journal of Geophysical Research: Space Physics*, *121*(5), 4119–4134. https://doi.org/10.1002/2016ja022427

von Papen, M., Saur, J., & Alexandrova, O. (2014). Turbulent magnetic field fluctuations in Saturn's magnetosphere. *Journal of Geophysical Research: Space Physics*, *119*(4), 2797–2818. https://doi.org/10.1002/2013ja019542

Vörös, Z., Baumjohann, W., Nakamura, R., Runov, A., Volwerk, M., Asano, Y., et al. (2007). Spectral scaling in the turbulent Earth's plasma sheet revisited. *Nonlinear Processes in Geophysics*, *14*(4), 535–541. https://doi.org/10.5194/npg-14-535-2007

Vörös, Z., Baumjohann, W., Nakamura, R., Volwerk, M., & Runov, A. (2006). Bursty bulk flow driven turbulence in the Earth's plasma sheet. *Space Science Reviews*, *122*(1), 301–311. https://doi.org/10.1007/s11214-006-6987-7

Vörös, Z., Baumjohann, W., Nakamura, R., Volwerk, M., Runov, A., Zhang, T. L., & Reme, H. (2004). Magnetic turbulence in the plasma sheet. *Journal of Geophysical Research*, *109*(A11), A11215. https://doi.org/10.1029/2004ja010404

Vörös, Z., Nakamura, R., Sergeev, V., Baumjohann, W., Runov, A., Zhang, T. L., et al. (2008). Study of reconnection-associated multiscale fluctuations with cluster and double star. *Journal of Geophysical Research*, *113*(A7), A07S29. https://doi.org/10.1029/2007ja012688

Wu, H., Tu, C., He, J., Wang, X., & Yang, L. (2022). Consistency of von Karman decay rate with the energy supply rate and heating rate observed by parker solar probe. *The Astrophysical Journal*, *926*(5), 116. https://doi.org/10.3847/1538-4357/ac4413

Wu, H., Tu, C., Wang, X., He, J., & Wang, L. (2019). Dependence of 3D self-correlation level contours on the scales in the inertial range of solar wind turbulence. *The Astrophysical Journal Letters*, *883*(6), L9. https://doi.org/10.3847/2041-8213/ab3fb1

Wu, H., Tu, C., Wang, X., He, J., & Yang, L. (2020). Energy Supply for heating the slow solar wind observed by parker solar probe between 0.17 and 0.7 AU. *The Astrophysical Journal Letters*, *904*(6), L8. https://doi.org/10.3847/2041-8213/abc5b6

Wu, H., Tu, C., Wang, X., He, J., Yang, L., & Yao, S. (2021). Energy supply by low-frequency break sweeping for heating the fast solar wind from 0.3 to 4.8 AU. *The Astrophysical Journal*, *912*(6), 84. https://doi.org/10.3847/1538-4357/abf099

Young, D. T., Berthelier, J. J., Blanc, M., Burch, J. L., Coates, A. J., Goldstein, R., et al. (2004). Cassini plasma spectrometer investigation. *Space Science Reviews*, *114*(1–4), 1–112. https://doi.org/10.1007/s11214-004-1406-4

Zhang, J., Huang, S. Y., He, J. S., Wang, T. Y., Yuan, Z. G., Deng, X. H., et al. (2022). Three-dimensional anisotropy and scaling properties of solar wind turbulence at kinetic scales in the inner heliosphere: Parker solar probe observations. *The Astrophysical Journal Letters*, *924*(2), L21. https://doi.org/10.3847/2041-8213/ac4027

Zhang, J., Huang, S. Y., Sahraoui, F., Andrés, N., Yuan, Z. G., Jiang, K., et al. (2023). Topology of magnetic and velocity fields at kinetic scales in incompressible plasma turbulence. *Journal of Geophysical Research: Space Physics*, *128*(1), e2022JA031064. https://doi.org/10.1029/2022ja031064

Zimbardo, G., Greco, A., Sorriso-Valvo, L., Perri, S., Vörös, Z., Aburjania, G., et al. (2010). Magnetic turbulence in the geospace environment. *Space Science Reviews*, *156*(1), 89–134. https://doi.org/10.1007/s11214-010-9692-5